

Perfect coupling of light to surface plasmons by coherent absorption

Heeso Noh, Yidong Chong, A. Douglas Stone, and Hui Cao*

Department of Applied Physics, Yale University, New Haven, CT 06511

Abstract

We show theoretically that coherent light can be completely absorbed in a two-dimensional or three-dimensional metallic nanostructure by matching the frequency and field pattern of an incident wave to that of a localized surface plasmon resonance. This can be regarded as critical coupling to a nano-plasmonic cavity, or as an extension of the concept of time-reversed laser to the spaser. Light scattering is completely suppressed via impedance matching to the nano-objects, and the energy of incoming wave is fully transferred to surface plasmon oscillations and evanescent electromagnetic fields. Perfect coupling of light to nanostructures has potential applications to nanoscale probing as well as background-free spectroscopy and ultrasensitive detection of environmental changes.

PACS numbers: 73.20.Mf; 42.25.Bs; 42.25.Hz

A fundamental issue in nanophotonics is the efficient delivery of light into regions with subwavelength dimension, to enhance linear and nonlinear optical processes on the nanoscale. This is a formidable problem because light can normally only be focused down to microscale regions due to the diffraction limit. Various schemes have been developed to couple laser radiation to the nanoscale, e.g. using tapered optical fibers or metal tips. Typically, only a small fraction of the incident energy can be transferred to the local field, and the rest is scattered as a stray background. Moreover, it is usually impossible to excite a single desired mode of the nanostructure. Several recently-proposed schemes include using a tightly-focused beam to improve the coupling of light with a nanoscale object [1, 2], and enhancing optical absorption by matching the shape of a nanoparticle to the field structure of a tightly focused beam [3]. While significant improvements are demonstrated in numerical simulations, perfect coupling or absorption is still out of the reach. In this paper, we propose a method for full delivery of optical energy to individual resonances of subwavelength structures.

Our method is based on time-reversed lasing, or coherent perfect absorption (CPA), a generalization of the concept of critical coupling that has recently been developed and realized using a simple optical cavity [4, 5]. An ordinary cavity made of dielectric material cannot be much smaller than the wavelength of light, because resonant feedback cannot be established in a volume of linear dimension less than a half-wavelength in the medium. However, metallic nanostructures support well-known surface plasmon resonances. Recent work has demonstrated that these resonances can be exploited in composite structures that include dielectric gain material to build self-organized oscillations. Such systems, referred to as “spasers” (surface plasmon amplification by stimulated emission) [6–11], are nanoplasmonic counterpart of lasers (with photons being replaced by surface plasmons and resonant cavities by metallic nanoparticles). The cavity modes correspond to localized surface plasmon (LSP) resonances, which can be confined to subwavelength in all three dimensions. Surface plasmon oscillations may be coupled to light outside the metallic cavities, producing coherent emission. In the time-reversed process, the coherent radiation is switched to an incoming field with phase-conjugated wavefront, and the gain medium replaced by a loss medium. The time-reversal symmetry demands a complete absorption of the input light, i.e., a perfect conversion of propagating waves from the far-field zone to LSPs and associated evanescent waves in the near-field zone. The basic theory of coherent perfect absorption applies to spasers, just as to conventional lasers: if the presence of optical gain can move

a resonant pole of the electromagnetic scattering matrix onto the real-frequency axis, the time-reverse of the electromagnetic equations implies that an appropriate amount of loss would produce a zero of the scattering matrix for real incident electromagnetic waves [4, 5]. While the spaser requires a dielectric material with gain, the plasmonic CPA does not need a dielectric material with loss, as it can use the intrinsic loss of metal.

The perfect excitation of LSPs in metallic nanostructures is accompanied by the creation of giant local fields, which are useful for nanoscale linear and nonlinear optical probing and manipulation. The fact that incident light can in principle be completely absorbed, without reradiation, points to possible applications in background-free spectroscopy and microscopy. Furthermore, we will see that the CPA condition can be very sensitive to small changes in the environment, which points to applications in refractive index sensing and detection of small concentrations of target molecules. The plasmonic CPA (time-reversed spaser) is a general concept for nanoparticles of any shape or even for clusters, but we will illustrate it here with simple structures such as metallic nano-cylinders and nano-spheres.

Consider an infinite metallic cylinder of radius R and dielectric constant ϵ_1 , embedded in a dielectric medium ϵ_2 . We denote the cylinder axis by \hat{z} . The incident light is assumed to propagate in the plane perpendicular to \hat{z} , as does any scattered light. We take the convention that transverse electric (TE) polarization denotes an in-plane magnetic field, and transverse magnetic (TM) polarization denotes an in-plane electric field. The two polarizations do not mix upon scattering and can be treated separately. TE waves cannot excite LSPs in the metallic cylinder, because the electric fields are parallel to \hat{z} and do not generate surface charges. TM waves, which have magnetic fields parallel to \hat{z} , do couple to LSPs. Due to the cylindrical symmetry of the system, the in-plane angular momentum is conserved. The scattering matrix is therefore diagonal, and its eigenstates (including zero-scattering eigenstates) have well-defined azimuthal number m .

Outside the cylinder ($r > R$), the total magnetic field of a TM mode can be written in cylindrical coordinates as

$$H_z(r, \theta, z) = H_m^{(2)}(n_2kr)e^{im\theta} + sH_m^{(1)}(n_2kr)e^{im\theta}, \quad (1)$$

where $n_2 = \sqrt{\epsilon_2}$, $k = 2\pi/\lambda$, and λ is the vacuum wavelength. $H_m^{(1)}$ ($H_m^{(2)}$) is the m th-order Hankel function of the first (second) kind, and represents an outgoing (incoming) wave in the far-field. s is the scattering amplitude for this mode. Inside the metal cylinder ($r < R$),

the magnetic field is $H_z(r, \theta, z) = aJ_m(n_1kr)e^{im\theta}$, where J_m is the Bessel function of the first kind, $n_1 = \sqrt{\epsilon_1}$, and a is a normalization constant. By matching the fields at the metal/dielectric interface ($r = R$), we get

$$s = \frac{n_1 J_m(n_1 k R) H_m^{(2)'}(n_2 k R) - n_2 J_m'(n_1 k R) H_m^{(2)}(n_2 k R)}{n_2 J_m'(n_1 k R) H_m^{(1)}(n_2 k R) - n_1 J_m(n_1 k R) H_m^{(1)'}(n_2 k R)}, \quad (2)$$

where J' (H') is the first-order derivative of the Bessel (Hankel) function. For CPA, the scattered wave vanishes ($s = 0$), which corresponds to the condition

$$n_1 J_m(n_1 k R) H_m^{(2)'}(n_2 k R) = n_2 J_m'(n_1 k R) H_m^{(2)}(n_2 k R). \quad (3)$$

This is the CPA condition for the whispering-gallery resonances of a dielectric cylinder. Now for a metal cylinder with $Re[\epsilon_1] < 0$, we can obtain solutions with $kR \ll 1$.

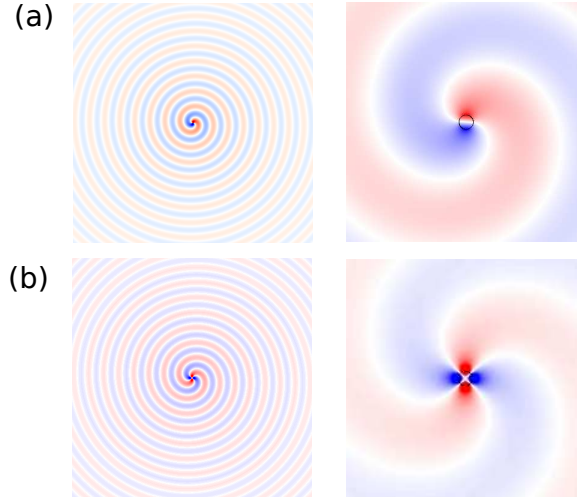


FIG. 1. Field patterns for CPA with a metallic nano-cylinder. Left column: spatial distribution of magnetic field H_z for perfect coupling of a TM-polarized incident wave to a LSP resonance. For (a), $m = 1$ and $\epsilon_1 = -1.14 + 0.158i$. For (b), $m = 2$ and $\epsilon_1 = -1.03 + 0.00162i$. In both cases, $kR = 0.3$ and $\epsilon_2 = 1$. Right column: expanded view of the field distributions in the vicinity of the cylinder, showing the buildup of strong local fields.

Figure 1(a) plots a solution for $m = 1$, $kR = 0.3$, $\epsilon_1 = -1.14 + 0.158i$, and $\epsilon_2 = 1.0$. The incoming wave spirals into the metallic cylinder, with zero scattered field. The radius of the cylinder R is much smaller than λ . Figure 1(b) shows another solution for $m = 2$, $kR = 0.3$, $\epsilon_1 = -1.03 + 0.00162i$, and $\epsilon_2 = 1.0$. An expanded view of the field pattern reveals the buildup of a strong local field at the cylinder surface. The propagating waves

from the far-field are completely converted to LSP oscillations and evanescent waves in the near-field.

A similar phenomenon can be realized in a three-dimensional (3D) metal sphere. Under spherical symmetry, LSP modes exist only for TM polarization (the radial component of the magnetic field vanishes). The CPA condition is obtained following procedures similar to the above, and can be expressed as

$$\epsilon_1 j_l(y_0) \frac{\partial [x h_l^{(2)}(x)]}{\partial x} \Bigg|_{x=x_0} = \epsilon_2 h_l^{(2)}(x_0) \frac{\partial [y j_l(y)]}{\partial y} \Bigg|_{y=y_0}, \quad (4)$$

where $x = \sqrt{\epsilon_2} k r$, $y = \sqrt{\epsilon_1} k r$, $x_0 = \sqrt{\epsilon_2} k R$, $y_0 = \sqrt{\epsilon_1} k R$, R is the radius of the metal sphere, ϵ_1 and ϵ_2 are the dielectric constants of the metal sphere and dielectric host medium respectively. j_l is the l th-order spherical Bessel function, and $h_l^{(2)}$ the spherical Hankel function of the second kind.

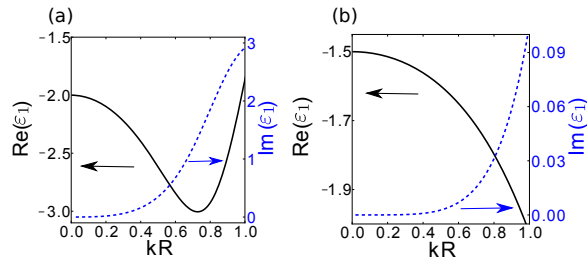


FIG. 2. CPA solution for a metal sphere in free space. Real part (left vertical axis) and imaginary part (right vertical axis) of the dielectric constant of metal as a function of kR for perfect coupling of impinging light to the LSP modes with $l = 1$ (a) and $l = 2$ (b). CPA is possible for an arbitrary small sphere with finite values of refractive index and absorption coefficient.

We consider a metallic sphere in free space ($\epsilon_2 = 1.0$). In order to generate a CPA resonance at a given frequency, one must tune both the real part and the imaginary part of ϵ_1 [4]. Instead of showing specific plasmonic CPA resonances at given values of kR , we show in Fig. 2 the continuous variation of the complex “CPA dielectric constant” under variation of kR , for two LSP resonances with $l = 1$ and 2. As can be seen, plasmonic CPA resonances can be realized for an arbitrarily small metal sphere. When $R \rightarrow 0$, $Re[\epsilon_1] \rightarrow -2.0$ and $Im[\epsilon_1] \rightarrow 0$ for $l = 1$. This corresponds to the quasi-static limit of the LSP resonance. For $l = 2$, $Re[\epsilon_1] \rightarrow -1.5$ and $Im[\epsilon_1] \rightarrow 0$ as $R \rightarrow 0$. This solution again gives a vanishing $Im[\epsilon_1]$ in the quasi-static limit. As noted above, perfect absorption can

be understood as a generalization of the “critical coupling” [12, 13] concept. For a LSP resonance, critical coupling means the rate of radiative loss is equal to that of dissipative loss. Under time reversal, radiative loss becomes radiative gain, and the dissipation of energy is fully compensated by the illuminating light. Since the radiative loss for a quasi-static resonance is extremely small, the dissipative loss in the nano-sphere would have to be equally small to achieve perfect absorption.

Such low dissipative loss is not typically achievable for a solid metal nanoparticle. For example, when the dispersive dielectric constant of gold (Au) [14] is inserted into Eq. 4, one finds that the smallest achievable value of kR is 0.91 at $\lambda = 535$ nm and $l = 2$. We therefore consider a composite silica core - gold shell structure, shown schematically in the inset of Fig. 3. The core sphere has radius R_c and the shell’s outer radius is R . As the gold shell gets thinner, the fraction of metal decreases and the dissipative loss of the system is reduced. As shown in the main panel of Fig. 3, the minimum achievable value of kR for CPA decreases as R_c/R increases. At the same time, the LSP resonance shifts to longer wavelengths where the metal loss is lower. For example, when $R_c/R = 0.9$ and $R = 63$ nm, the CPA condition is reached at $\lambda = 771$ nm.

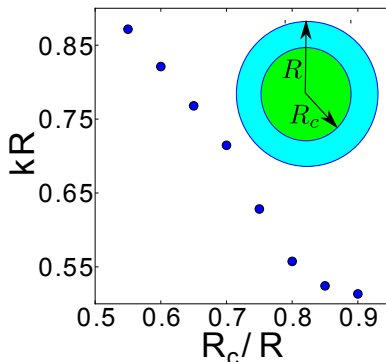


FIG. 3. CPA for silica core - gold shell structures. Main panel: minimal value of kR as a function of R_c/R for $l = 1$. Inset: a schematic diagram of the core-shell structure. The total structure size R reduces as the metal shell gets thinner.

Although we have only presented calculations for cylindrical and spherical structures, the time-reversal argument implies that similar CPA phenomena can occur in more complex structures with LSP resonances, so long as there is an appropriate amount of dissipative loss. It might appear that CPA cannot occur for dark (non-radiative) plasmonic resonances.

However, a typical dark mode has only vanishing electric dipole moment; radiation can still occur in higher multipole moments (e.g. magnetic dipole and electric quadrupole). Hence, it is possible in principle to achieve CPA by coupling to a dark mode, as long as the radiative coupling of the dark mode is not completely vanishing; however, the high quality (Q) of the dark mode imposes the requirement of very low dissipation.

Compared to a spaser, a significant difference and also an advantage of a perfect absorber of the present type is that incident light can be coupled to any LSP resonance of the structure—not just the low-loss ones. Just as in a laser, the spaser usually oscillates in the LSP resonances with low loss, which saturate the gain, making it difficult for higher-loss resonances to reach threshold. In the time-reversed (absorber) case, the incident wave can be perfectly absorbed by any LSP resonance so long as its frequency and field pattern match that particular resonance. In the regime where absorption is a linear process, we can simultaneously achieve perfect absorption for several modes by superimposing the corresponding incident wave patterns.

The CPA phenomenon is extremely sensitive to variations in the incident wave or the dielectric environment. Small changes can violate the perfect-absorption condition, resulting in a dramatic increase of the scattered intensity. Figure 4(a) plots the scattered intensity of the outgoing wave, $|s|^2$, for a metallic cylinder as a function of the incoming light frequency k . As k deviates from a LSP resonance frequency, the scattered light intensity increases rapidly from zero. The spectral width of the CPA resonance is $\Delta k/k \simeq 0.1$, and it is determined by the dissipative loss of the LSP mode. This result is promising for application to background-free spectroscopy. A similar effect is found for a tiny change in refractive index or absorption coefficient of the surrounding material, as shown in Fig. 4(b) for a variation in n_2 . Hence, the effect may also be useful for ultrasensitive detection of environmental changes.

In the recent development of metamaterial absorbers, impedance matching has been used to eliminate reflection of a plane wave from the front surface, with transmission minimized by the use of multiple absorbing layers or a mirror at the back surface of the sample [15–19]. Although the dimension of each unit cell is subwavelength, the entire medium is macroscopic. CPA, which is a generalization of the concept of impedance matching to arbitrary geometries and dimension, is applied here to a single subwavelength object in free space. By matching the incident field pattern to the radiation pattern of a LSP resonance, 100% coupling efficiency is reached, and light scattering in all directions is eliminated. However,

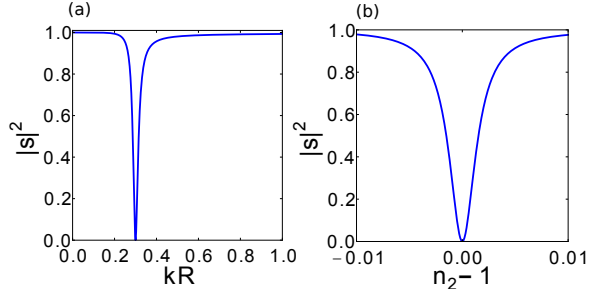


FIG. 4. Sensitivity of CPA to variations in the incident wave and the dielectric environment. (a) Normalized intensity $|s|^2$ of scattered light versus the frequency k of the incident light (normalized by $1/R$, where R is the radius of the metallic cylinder). CPA is reached at $kR = 0.3$ via resonant excitation of the LSP resonance with $m = 2$. The spectral width of the dip in $|s|^2$ is determined by the dissipative loss of the LSP resonance. (b) $|s|^2$ as a function of the change in refractive index $n_2 - 1$ of the dielectric material surrounding the metallic cylinder. CPA happens at $n_2 = 1$. A tiny derivation of n_2 from one causes a dramatic growth of the scattered light intensity.

the input field for perfect-coupling to a nanosphere is an angular momentum eigenstate, which must converge onto it from all directions, something not easy to do experimentally. To simplify the experimental requirements, it will likely be useful to strongly break the rotation symmetry, e.g. by employing ellipsoids or nano-rods, in order to approach the resonance condition with a more directional input wave pattern. Similar directional emission of lasing from deformed dielectric microcavities has been extensively studied [20–22], which could benefit the design of metallic nanoabsorbers.

The CPA mechanism differs from the spatial-temporal localization of optical energy in a nanoplasmonic system by time-reversal [23]. In the latter case, a short pulse is launched from a point in the near field and the radiation in the far field is recorded. Time-reversal of the radiated pulse leads to concentration of input energy at the position of the initial source at a time corresponding to the end of the excitation pulse. Afterwards, the field passes through the focal point and diverges. The input energy is not completely absorbed at the focus, unless a time-reversed source is placed there [24]. In contrast, the CPA mechanism does not need a coherently-driven source. Instead it sets up a perfect “trap” for the incident light by matching it to a resonance of the system. Thus it works only for coherent light at the resonant frequency.

In summary, we have demonstrated the possibility of coherent perfect absorption of light

by nano-scale metallic objects, equivalent to time-reversing the spaser and perfect coupling to localized surface plasmons. The required input field must be monochromatic and coherent, and the system must have an optimal loss equivalent to the critical coupling condition. The required incident waveform depends on the shape of the nano-scale object; for spherical or cylindrical structures that are considered here, it is simply a converging spherical or cylindrical TM wave. Other structures may require a complex superposition of spherical waves, the form of which requires further study.

We thank Profs. Mathias Fink, Geoffroy Lerosey, and Rupert F. Oulton for stimulating discussions. This work is funded by the NSF Grants DMR-0908437 and ECCS-1068642.

* hui.cao@yale.edu

- [1] G. Zumofen, N. M. Mojarad, V. Sandoghdar, and M. Agio, *Phys. Rev. Lett.* **101**, 180404 (2008).
- [2] N. M. Mojarad, V. Sandoghdar, and M. Agio, *J. Opt. Soc. Am. B* **25**, 651 (2008).
- [3] A. Normatov, B. Spektor, Y. Leviatan, and J. Shamir, *Opt. Express* **19**, 8506 (2011).
- [4] Y. D. Chong, L. Ge, H. Cao, and A. D. Stone, *Phys. Rev. Lett.* **105**, 053901 (2010).
- [5] W. Wan, Y. Chong, L. Ge, H. Noh, A. D. Stone, and H. Cao, *Science* **331**, 889 (2011).
- [6] D. J. Bergman and M. I. Stockman, *Phys. Rev. Lett.* **90**, 027402 (2003).
- [7] N. I. Zheludev, L. S. Prosvirnin, N. Papasimakis, and A. V. Fedotov, *Nature Photon.* **2**, 351 (2008).
- [8] M. A. Noginov, G. Zhu, A. M. Belgrave, R. Bakker, V. M. Shalaev, E. E. Narimanov, S. Stout, E. Herz, T. Suteewong, and U. Wiesner, *Nature* **460**, 1110 (2009).
- [9] R. F. Oulton, V. J. Sorger, T. Zentgraf, R.-M. Ma, C. Gladden, L. Dai, G. Bartal, and X. Zhang, *Nature* **461**, 629 (2009).
- [10] M. I. Stockman, *Phys. Rev. Lett.* **106**, 156802 (2011).
- [11] S. Wuestner, A. Pusch, K. L. Tsakmakidis, J. M. Hamm, and O. Hess, *Phys. Rev. Lett.* **105**, 127401 (2010).
- [12] M. Cai, O. Painter, and K. J. Vahala, *Phys. Rev. Lett.* **85**, 74 (2000).
- [13] A. Yariv, *IEEE Photon. Technol. Lett.* **14**, 483 (2002).
- [14] P. B. Johnson and R. W. Christy, *Phys. Rev. B* **6**, 4370 (1972).

- [15] N. I. Landy, S. Sajuyigbe, J. J. Mock, D. R. Smith, and W. J. Padilla, *Phys. Rev. Lett.* **100**, 207402 (2008).
- [16] Y. Avitzour, Y. A. Urzhumov, and G. Shvets, *Phys. Rev. B* **79**, 045131 (2009).
- [17] B. Wang, T. Koschny, and C. M. Soukoulis, *Phys. Rev. B* **80**, 033108 (2009).
- [18] N. Liu, M. Mesch, T. Weiss, M. Hentschel, and H. Giessen, *Nano Lett.* **10**, 2342 (2010).
- [19] A. Polyakov, S. Cabrini, S. Dhuey, B. Harteneck, P. J. Schuck, and H. A. Padmore, *Appl. Phys. Lett.* **98**, 203104 (2011).
- [20] J. U. Nockel and A. D. Stone, *Nature* **385**, 45 (1997).
- [21] J. Wiersig and M. Hentschel, *Phys. Rev. Lett.* **100**, 033901 (2008).
- [22] Q. H. Song and H. Cao, *Phys. Rev. Lett.* **105**, 053902 (2010).
- [23] X. Li and M. I. Stockman, *Phys. Rev. B* **77**, 195109 (2008).
- [24] J. de Rosny and M. Fink, *Phys. Rev. Lett.* **89**, 124301 (2002).